Reduced-order trajectory piecewise-linear models for nonlinear computational fluid dynamics

D. Gratton* and K. Willcox†
Massachusetts Institute of Technology
Cambridge, MA 02139

Abstract

A trajectory piecewise linear (TPWL) approach is developed for a computational fluid dynamics (CFD) model of the two-dimensional Euler equations. The approach uses a weighted combination of linearized models to represent the nonlinear CFD system. The proper orthogonal decomposition (POD) is then used to create a reduced-space basis, onto which the TPWL model is projected. This projection yields an efficient reduced-order model of the nonlinear system, which does not require the evaluation of any full-order system residuals. The method is applied to the case of flow through an actively controlled supersonic diffuser. With an appropriate choice of linearization points and POD basis vectors, the method is found to yield accurate results, even for cases with significant shock motion. In this draft paper, TPWL results are presented for the full CFD system. In the final paper, reduced-order TPWL results will also be included.

Introduction

Computational fluid dynamics (CFD) is now widely used throughout the fluid dynamics community. It produces accurate models for many problems of interest, although the cost of obtaining the solution may be prohibitive for some applications. In particular, this cost becomes critical for aeroelastic or active flow control design applications. Model order reduction techniques provide a way to systematically determine low-order models that capture the relevant dynamics of the CFD model while being computationally very efficient. These techniques have been applied successfully for a range of fluid dynamic applications.[1,5,7,11,23]

While model reduction is now a well established approach for large linear systems, the problems that arise for consideration of nonlinearity remain a challenging task. A number of linear reduction techniques have been extended to the nonlinear case with varying success. One approach to generate reduced-order models for nonlinear systems is a polynomial (Taylor) expansion of system's nonlinearity, and subsequent application of Krylov projection.[2,14,17] However, the main drawbacks of those methods are that they are limited to applications with "small" input disturbances, or more generally called weakly nonlinear systems, and that the quadratic and higher order expansion terms are very expensive to compute.

The proper orthogonal decomposition (POD) is a widely used method of reduction for CFD applications, and has been applied to nonlinear systems. However, in these applications, the issue of an efficient representation of the nonlinearity in the reduced-order model is inadequately addressed. While the resulting nonlinear models do have a reduced number of states, they still require flux evaluations of the original high-order CFD model.

In Rewienski, a trajectory piecewise-linear (TPWL) scheme, is developed.[18,19] This technique aims to address some fundamental issues presented earlier, i.e. overcoming restrictions of weak nonlinearity and creating a cost-efficient representation of the system's nonlinearity. By using a weighted combination of various linear models, a broader range of the nonlinear space is spanned compared with using a single model. In addition, the TPWL systems allows an efficient representation of the reduced-order model. A number of good results have been obtained with nonlinear analogue circuits and micromachined devices.[18,19]

This paper considers the TPWL approach in

*Department of Aeronautics and Astronautics, Room 37-442, MIT, Cambridge, MA 02139, dgratton@mit.edu
†Assistant Professor of Aeronautics and Astronautics, Room 37-447, MIT, Cambridge, MA 02139, kwillcox@mit.edu, Member AIAA

conjunction with a POD-based reduction for CFD applications. In the next section, the CFD model is described, considering in particular the case of flow through an actively controlled supersonic diffuser. The general model reduction framework is then established, followed by a description of the TPWL approach and its application to the reduced-order models. Finally, results are presented and conclusions are drawn.

Computational Model

The computational model is based on the case of flow through a supersonic diffuser; however, the TPWL methodology is general and could be applied to any CFD model. Figure 1 shows the Mach contours at steady-state conditions inside the fixed geometry of a supersonic diffuser that operates at a freestream Mach number of 2.2. In steady-state operation, a shock forms downstream of the throat; however in practice, the incoming supersonic flow is subject to perturbations, such as atmospheric density disturbances. Such perturbations in the flow may cause the shock to move upstream of the throat, and eventually to be expelled from the diffuser. This phenomenon, known as inlet unstart, causes huge losses in engine performance and thus is highly undesirable. In order to prevent inlet unstart, an active control mechanism of the shock is required.

Fig. 1 Mach contours for steady flow through supersonic diffuser. Steady-state inflow Mach number is 2.2.

Figure 2 presents the schematic of the actuation mechanism. Incoming flow with possible disturbances enter the inlet and is sensed using pressure sensors. The controller then adjusts the bleed upstream of the throat in order to control the position of the shock and to prevent it from moving upstream.

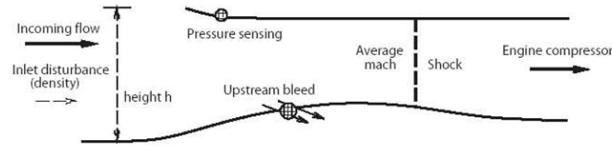

Fig. 2 Supersonic diffuser active flow control problem setup.

Nonlinear CFD Model

The full nonlinear solution of the entire flow distribution in the inlet can be obtained using a CFD model. Here, the problem is assumed to be two-dimensional, compressible and inviscid, thus the solution is governed by the Euler equations. The discrete Euler equations are derived from the integral form of the unsteady, two-dimensional equations, which are the usual statements of mass, momentum, and energy:

$$\begin{aligned}
\frac{\partial}{\partial t}\iint \rho dV \quad &+ \quad \oint dm = 0 \\
\frac{\partial}{\partial t}\iint \rho\vec{Q} dV \quad &+ \quad \oint \vec{Q} dm + \oint p d\vec{A} = 0 \\
\frac{\partial}{\partial t}\iint \rho E dV \quad &+ \quad \oint H dm = 0
\end{aligned} \qquad (1)$$

where the flow variables are the density, ρ, the total velocity vector, $\vec{Q}$, the pressure, p, the energy, E, and the total enthalpy, H. The quantity $dm = \rho\vec{Q}\cdot d\vec{A}$ is the mass flux element across the moving conservation cell boundary, $d\vec{A} = dA\cdot\hat{n}$, where dA is a surface element and $\hat{n}$ is a unit vector pointing outward from the control volume. The discrete Euler equations approximate the integral form of the continuous Euler equations on small control volumes or control cells. The flow solver is fully described in Drela[3] and Lassaux,[11] and uses as state variables the streamwise component of the velocity, q, the normal component of the velocity, $q_\perp$, the density, ρ, and the total enthalpy, H.

Using a structured grid for spatial discretization, the discrete Euler equations can be represented as a nonlinear dynamical system of the form:

$$\begin{aligned}
\dot{x}(t) \quad &= \quad f(x(t), u(t)) \\
y(t) \quad &= \quad g(x(t))
\end{aligned} \qquad (2)$$

where $x(t) \in R^n$ is a generalized state vector containing the n unknown flow quantities, q, $q_\perp$, ρ and H, at each point in the computational grid, f is a nonlinear vector-valued function, $u(t) \in R^l$ is the input to the system, $y(t) \in R^k$ contains the system outputs, which are defined by the nonlinear function g.

Reduced Space Basis

A reduced-order model can be obtained by considering a projection of the state vector x

$$x(t) = V\hat{x}(t) \tag{3}$$

where $\hat{x}(t) \in R^m$ is the reduced-order state vector, containing the time-dependent amplitudes of m basis vectors, contained in the columns of the matrix V. The basis vectors must be selected appropriately, so that the state x can be accurately represented in the reduced space. In this work, POD is used to determine the basis vectors as follows.

First, N snapshots are obtained from a CFD calculation, where each snapshot corresponds to a flow solution at a particular instant in time. The correlation matrix R is formed by computing the inner product between every pair of snapshots

$$R_{ij} = \frac{1}{N}\left(x^{(i)}, x^{(j)}\right) \tag{4}$$

where $x^{(i)}$ is the flow solution at a time $t^{(i)}$ and $\left(x^{(i)}, x^{(j)}\right)$ denotes the inner product between $x^{(i)}$ and $x^{(j)}$. The eigenvalues λ_i and eigenvectors $\psi^{(i)}$ of R are then computed. The magnitude of the j^{th} eigenvalue, λ_i, describes the relative importance of the j^{th} POD basis vector, V_j, which is computed by

$$V_j = \sum_{i=1}^{N} \psi_i^{(j)} x^{(i)} \tag{5}$$

where $\psi_i^{(j)}$ denotes the i^{th} component of the j^{th} eigenvector.

This orthonormal set of POD basis vectors can be used to project the solution onto the reduced-space basis using (3). The size of $\hat{x}$, m, will depend on the number of components taken in the basis V. This number can be chosen using a heuristic criterion based on capturing a sufficiently large amount of the "energy" contained in the snapshot collection. The energy e_j captured by each mode j is given by the POD eigenvalues as

$$e_j = \frac{\lambda_j}{\sum_{i=1}^{N} \lambda_i} \tag{6}$$

Applying this projection to the nonlinear system (2), the resulting reduced-order model is of the form

$$\begin{aligned} \dot{\hat{x}}(t) &= V^T f(V\hat{x}(t), u(t)) \\ \hat{y}(t) &= g(V\hat{x}(t)) \end{aligned} \tag{7}$$

While the system (7) has a reduced number of states, it still requires evaluation of the full order flux term $f(\cdot)$. To obtain a truly reduced model, a more efficient representation of the nonlinearity in the reduced space is required.

Linearized Models

Efficient linearized models can be extracted from the system (2) by using a polynomial expansion of the nonlinearity, or more specifically a Taylor expansion about some state (x_i, u_i), which, following Phillips,[16] expands f as:

$$\begin{aligned} f(x,u) &= f(x_i,u_i) + A_i(x - x_i) + B_i(u - u_i) \\ &\quad + \frac{1}{2}W_i(x - x_i) \otimes (x - x_i) + \dots \end{aligned} \tag{8}$$

where $\otimes$ is the Kronecker product, and A_i and W_i are, respectively, the Jacobian and the Hessian of $f(\cdot)$ evaluated at the state (x_i, u_i). The matrix $B_i = \frac{\partial f}{\partial u}$ is also evaluated at (x_i, u_i). Dropping the quadratic and higher terms of (8), the nonlinear system (2) can be linearized about a given state to yield a state-space model of the form:

$$\begin{aligned} \dot{x}(t) &= A_i x(t) + B_i u(t) + (f(x_i, 0) - A_i x_i(t)) \\ y(t) &= C_i x(t) \end{aligned} \tag{9}$$

where $C_i = \frac{\partial g}{\partial x}$ is also evaluated at (x_i, u_i) and u_i is assumed to be zero.

The vector of unknowns $x(t)$ can be written as

$$x(t) = x_i + x_i'(t) \tag{10}$$

where x_i, fixed in time, is the value of state vector x at the linearization point i, and $x_i'(t)$ contains the perturbation of the n unknown flow quantities about that linearization point x_i. The linearized equation (9) can then be expressed as

$$\begin{aligned} \dot{x_i}'(t) &= A_i x_i'(t) + B_{1i} u(t) + B_{2i} \\ y(t) &= C_i x_i'(t) + C_{0i} \end{aligned} \tag{11}$$

where $B_{2i} = f(x_i, 0)$ and $C_{0i} = C_i x_i$.

The linearized system (11) is efficient for time computations, but remains too large for applications such as controller design. A reduced-order linearized model can be obtained by applying the projection (3) to the system (11) yielding

$$\begin{aligned}\frac{d}{dt}\hat{x}'_i(t) &= \hat{A}_i\hat{x}'_i(t) + \hat{B}_{1i}u(t) + \hat{B}_{2i} \\ \hat{y}_i(t) &= \hat{C}_i\hat{x}'_i(t) + \hat{C}_{0i}\end{aligned} \quad (12)$$

where the reduced-order matrices are given by

$$\begin{aligned}\hat{A}_i &= V^T A_i V \\ \hat{B}_{1i} &= V^T B_{1i} \\ \hat{B}_{2i} &= V^T B_{2i} \\ \hat{C}_i &= C_i V \\ \hat{C}_{0i} &= C_{0i} V\end{aligned} \quad (13)$$

The system (12) is truly reduced since the projections can be carried out a priori and no CFD-order computations are required for simulation. However, the linearized models do not accurately capture nonlinear behavior. The next section will therefore focus on finding a suitable way to capture nonlinear behavior within the reduction framework.

Trajectory Piecewise-Linear Scheme

In Rewienski,[19] an efficient, approximate method to represent nonlinear circuit systems is presented and tested. It is proposed that by using a weighted combination of multiple linear models, nonlinear behavior can be modelled. The linear models are obtained via linearization of the nonlinear system at different solutions in time. An approximation to the nonlinear system can then be obtained by using a weighted combination of the closest linear models to the current solution in time.

Figure 3 presents a two-dimensional conceptual view of a series of linearized models. Plotted are four linearization points, x_1, x_2, x_3 and x_4, along a "training trajectory", which is obtained using a simulation of the nonlinear system. The range of validity of each of the corresponding linearized models is denoted by the circles. In order to capture the most relevant dynamics of the system, the range of inputs simulated for the training trajectory should reflect dynamics of interest for the application at hand. For instance, in Figure 3, trajectories such as B and C will be well represented by the set of linear models, while trajectories D and E may demonstrate poor results, since they lie beyond the range of validity.

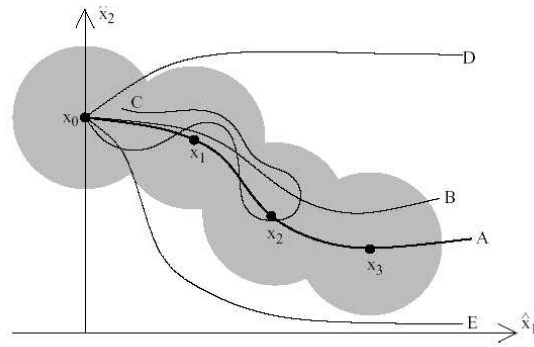

Fig. 3 Collection of linearization points x_0, x_1, x_2 and x_3 in a 2D state space. Circles denotes suitable region for use of each linearization points. Trajectory A is called the training trajectory. Figure from Rewienski .[19]

The linearization points can be chosen using the following approach. Consider N snapshots, taken from the training trajectory. The algorithm compares each pair of snapshots by computing the two-norm of the distance between them. When this difference is larger than a specified criterion, δ_{min}, a new linearization point is selected. The value of δ_{min} sets the distance between subesquent linearization points; therefore, lowering its value implies increasing the number of models in the system. This approach is described by the pseudo-algorithm below, which takes as inputs δ_{min} and the matrix U containing N CFD snapshots

$$U = \{x^{(0)}, x^{(1)}, ..., x^{(N-1)}\} \quad (14)$$

and returns the vector $linPt$, which contains the column index in U of the selected linearization points.

Algorithm 1
(Choice of linearization points on the fly)
Function linPt = linearizationPoint(U, δ_{min})

$N = size(U, 2)$

$linPt = [0]$

for $i = 1 : N$

$k = size(linPt)$
$\delta = \infty$
for $j = 1 : k$
$\delta' = \frac{\|U^{(i)} - U^{(linPt(j))}\|}{\|U^{(linPt(j))}\|}$
$\delta = min[\delta, \delta']$

end

if $(\delta > \delta_{min})$

$linPt = [linPt\ i]$

end

end

With the set of linear models created, a TPWL scheme can be assembled in order to model nonlinearity. Consider a weighted combination of s linearized models of system (11)

$$\begin{aligned}\sum_{i=0}^{s-1}\tilde{\omega}_i(x)\Big\{\dot{x}_i'(t) &= A_i x_i'(t) + B_{1i}u(t) + B_{2i}\Big\}\\ \sum_{i=0}^{s-1}\tilde{\omega}_i(x)\Big\{y_i(t) &= C_i x_i'(t) + C_{0i}\Big\}\end{aligned} \tag{15}$$

where $\tilde{\omega}_i(x)$ are weights depending on the value of the perturbation about the linearization point x_i. It is assumed that for all x, $\sum_{i=0}^{s-1}\tilde{\omega}_i(x) = 1$. The weights $\tilde{\omega}_i(x)$ are then obtained using the distance $\|x(t) - x_i\|$ between the linearization point x_i and the current solution $x(t)$. The following procedure, following Rewienski,[19] ensures that the "dominant" model i is that corresponding to the linearization point x_i that is the closest to the current state of the system:

Algorithm 2 (Weights computation)

1. For $i = 0, ..., (s-1)$ compute:
   $d_i = \|x(t) - x_i\|_2$.
2. $[m, k] = min\{d_i : i = 0, ..., (s-1)\}$.
3. a) For $i = 0, ..., (s-1)$ compute:
      $\tilde{\omega}_i = (exp(d_i)/m)^{-25}$.
      or
   b) For $i = 0, ..., (s-1), \tilde{\omega}_i = 0$
      $\tilde{\omega}_k = 1$.
4. Normalize $\tilde{\omega}_i$.

First, Algorithm 2 obtains the difference d_i between the current state $x(t)$ and the linearization point x_i. The minimum distance is given by m and corresponds to the model with index k. Then, the weights can be computed in two different ways. The first method shows a weighted sum strongly concentrated on the closest model, while the second uses only the closest model at the time. As will be presented later, each formulation yields slightly different results. The last step in the algorithm ensures that the summation of the s weights is unity.

Reduced-Order TPWL Model

Using the TPWL representation of the nonlinear system, an efficient reduced-order model can now be obtained using the projection (3) applied to (15), yielding a reduced-order TPWL model as follows.

$$\begin{aligned}\sum_{i=0}^{s-1}\tilde{\omega}_i(\hat{x})\Big\{\frac{d}{dt}\hat{x}_i'(t) &= \hat{A}_i\hat{x}_i'(t) + \hat{B}_{1i}u(t) + \hat{B}_{2i}\Big\}\\ \sum_{i=0}^{s-1}\tilde{\omega}_i(\hat{x})\Big\{\hat{y}_i(t) &= \hat{C}_i\hat{x}_{0i}'(t) + \hat{C}_{0i}\Big\}\end{aligned} \tag{16}$$

As in the linear case, this representation is efficient, since all reduced-order matrices in (16) can be precomputed. Note also that the weights ω_i are computed as a function of the reduced-order state $\hat{x}$. The TPWL approach fits well within the context of POD-based model reduction, since a simulation of the nonlinear system can provide both the snapshots for computation of the POD basis vectors and also a set of instantaneous flow states from which to select the linearization points.

The final TPWL reduction approach can be summarized as follows. First, simulate the nonlinear CFD model for a range of forcing functions and conditions that are representative of the application at hand. Second, from the resulting snapshot collection, calculate a set of POD basis vectors. Third, from the same snapshot collection, select a set of linearization points using Algorithm 1. Fourth, using the dominant POD basis vectors, project each linearized model to obtain a set of reduced-order linear state-space systems. Finally, combine these low-order state-space systems using the TPWL representation.

This approach will now be demonstrated for the case of flow through the supersonic diffuser shown in Figure 2. Both full-order and reduced-order TPWL models will be constructed, and the results compared with full nonlinear CFD outputs.

Results

A number of test cases will be presented to demonstrate the TPWL methodology. In all

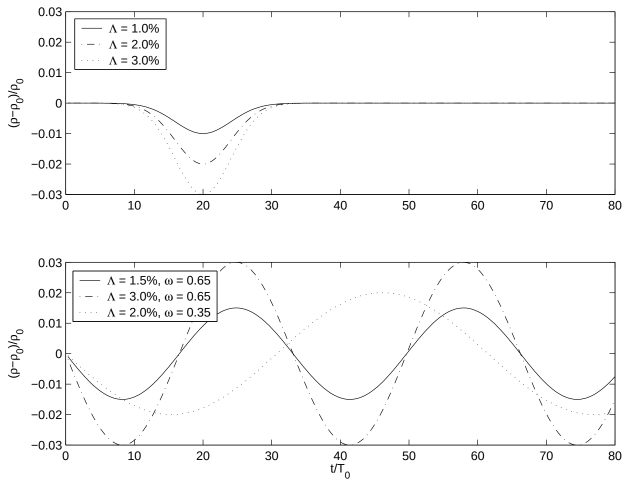

Fig. 4 Incoming density disturbances. Top: Gaussian distributions. Bottom: sinusoidal distributions.

Case	Λ	t_{peak}	α
1	1%	20	$0.03f_0^2$
2	2%	20	$0.03f_0^2$
3	3%	20	$0.03f_0^2$

Table 1 Data used for the Gaussian distribution.

cases, the input considered is an incoming density disturbance and the output of interest is the average Mach number at the throat of the diffuser. The six different temporal distributions considered for the input are presented in Figure 4, and vary temporally either with a Gaussian pulse or a sinusoidal distribution of various phases and amplitudes. The Gaussian distribution is described by

$$\rho'(t) = -\Lambda\rho_0 e^{-\alpha(t-t_{peak}/f_0)^2} \tag{17}$$

while the sinusoidal distribution is described by

$$\rho'(t) = -\Lambda\rho_0 \sin\omega_0 t \tag{18}$$

where the nominal frequency f_0 equals a_0/h, the inlet speed of sound divided by the height of the inlet, and the non-dimensional time, t_{peak}, sets the time at which the perturbation peaks. α sets how sharp will the perturbation be, while Λ corresponds to the amplitude of the perturbation. The parameter values corresponding to the six different input functions are presented in Tables 1 and 2.

Nonlinear CFD results are obtained by simulation of the full system, and snapshots at selected

Case	Λ	ω_0
4	1.5%	0.65
5	2%	0.35
6	3%	0.65

Table 2 Data used for the sinusoidal distribution.

δ_{min}	Case number			
	1	2	3	6
∞	1	1	1	1
0.030	1	3	4	7
0.020	2	4	8	16
0.015	3	6	16	31
0.012	4	11	23	41
0.010	5	16	28	50
0.008	6	20	34	70
0.006	12	29	48	100
0.005	15	36	56	118
0.004	20	42	69	147

Table 3 Number of models given by different values of δ_{min} for the three Gaussian distributions and for one of the Sinusoidal distribution.

timesteps are saved. Using Algorithm 2 for different values of δ_{min} and the snapshots just obtained, various sets of models are found. Table 3 shows the number of models as a function of the choice of δ_{min} for four of the cases, where each case was considered separately. For each case, it can be seen by how much the number of models grows as the distance between linearization points is decreased. By comparing the number of models for a given δ_{min}, one gains some insight to the importance of nonlinearity in each case. For example, a Gaussian distribution of 3% can be seen to introduce more nonlinearity into the system than one of 1%, requiring substantially more models for a given δ_{min}.

Full-Order TPWL Models

Once the linearization points have been determined, the validity of the TPWL representation must be tested. This was done by comparing nonlinear CFD results with those obtained using a full-order TPWL approximation as in Equation (15). The results using different sets of models from Table 3 are shown on Figure 5, where the average Mach number at the throat is plotted against time. Here, both the training trajectory and the disturbance were a Gaussian distribution of 3% amplitude. Figure 5 shows the

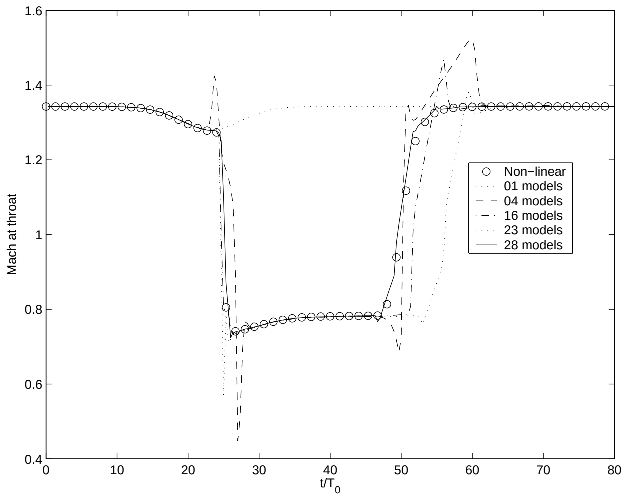

Fig. 5 Nonlinear response plotted against a weighted sum of various full linear models combinations for a Gaussian incoming disturbance of 3% amplitude. Training trajectory obtained from the same simulation.

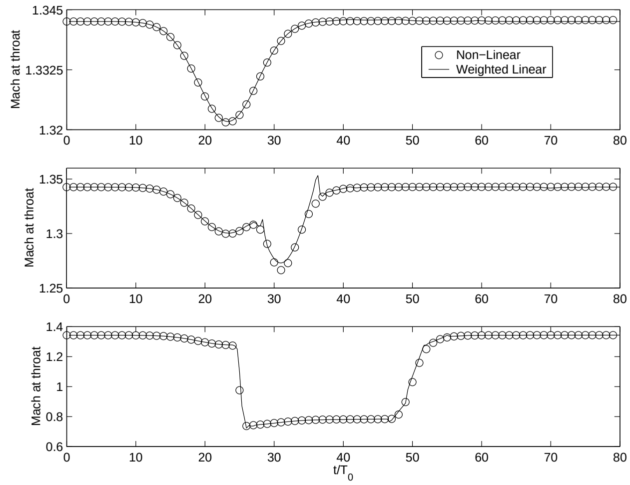

Fig. 6 Nonlinear response plotted against weighted sum of full linear models for a Gaussian incoming disturbance of various amplitudes. From top, amplitude of 1%, 2% and 3%. The training trajectory for each cases was the same as the simulation. $\delta_{min} = 0.01$

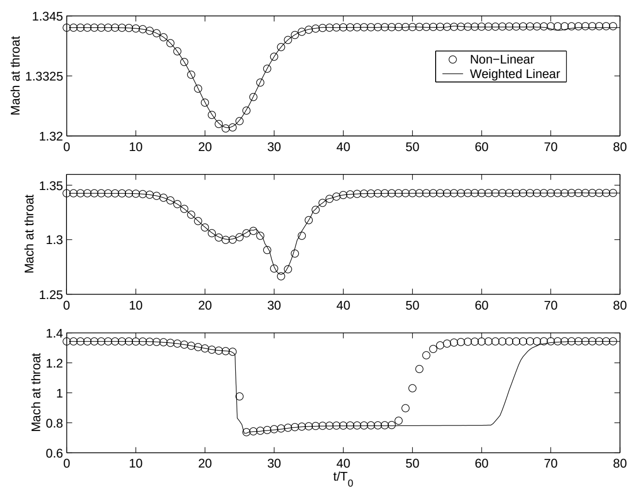

Fig. 7 Nonlinear response plotted against weighted sum of full linear models for a Gaussian incoming disturbance of various amplitudes. From top, amplitude of 1%, 2% and 3%. The training trajectory for each cases was the same as the simulation.$\delta_{min} = 0.005$

number of models needed to accurately represent the nonlinear behavior. It can be seen that only one linearized model cannot capture the nonlinear behavior of a shock. As the value of δ_{min} is decreased, the match improves with increasing number of models. It can be seen in Figure 5 that with 28 models ($\delta_{min} = 0.01$), the nonlinear CFD results are matched by the combination of full-order linear models.

Figures 6 and 7 show TPWL results for all of the Gaussian amplitudes, using values of δ_{min} equal to 0.01 and 0.005, respectively. For each case, the training trajectory corresponds to the desired incoming disturbance. Comparing these figures, one gains insight to the value of δ_{min} required in order to obtain a good match between the piecewise-linear combination of models and the nonlinear CFD. As Figure 5 shows, a minimum number of models is needed to capture a sufficiently high degree of nonlinearity. However, as Figure 7 demonstrates, taking too many models may cause undesirable results. In particular, oscillations may be observed or behavior may be inaccurately captured in sensitive regions. This is observed in the lower plot of Figure 7 at a time $t/T_0 \approx 50$ corresponding to the point at which the shock returns to a position downstream of the throat. These problems are further demonstrated in Figure 8, where even a small increase in the number of models leads to oscillations and inaccuracies in sensitive regions. Systematic strategies to avoid this behavior are the subject of ongoing research.

In the context of finding a reduced-order model that is valid over a range of flow conditions, the different input cases would not be considered separately. Rather, the snapshots from each would be combined to find a TPWL system that captures all training trajectories. To achieve this, all

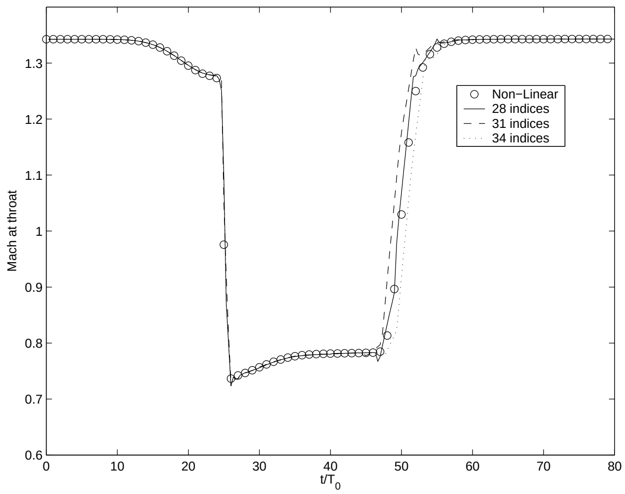

Fig. 8 Nonlinear response plotted against weighted sum of various full linear models combinations for a Gaussian incoming disturbance of 3% amplitude. Training trajectory obtained from the same simulation.

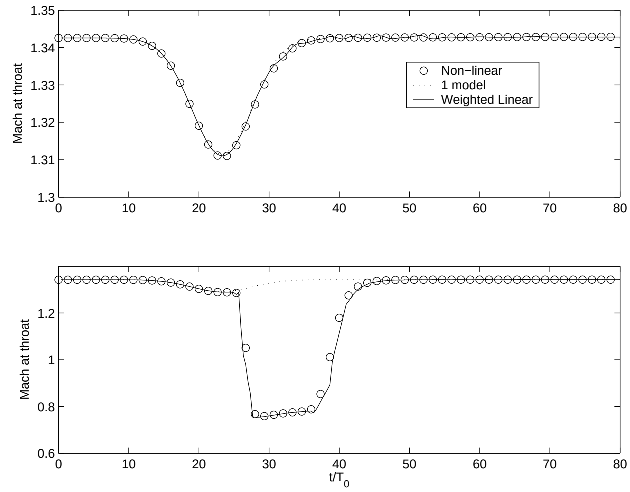

Fig. 9 Nonlinear response plotted against weighted sum of 67 full linear models. From top: Gaussian amplitude of 1.5% and 2.5%. Training trajectories obtained from incoming density disturbances of Gaussian amplitudes of 1%, 2% and 3%.

previous models obtained from the three different amplitudes of 1%, 2% and 3% were combined to form one large set of 67 models. This is, adding the 5, 35 and 27 models together, without repeating the steady state. Results for simulations of Gaussian amplitudes of 1.5% and 2.5% are shown on Figure 9. Note that these cases were not considered as part of the training trajectory set; however, they would be expected to fall within the range of validity of the existing ensemble. Very good agreement between the full nonlinear CFD and the set of combined models can be seen, as well as a dramatic improvement of the TPWL approach over using a single linearized system.

Reduced-Order TPWL Models

A number of parameters must be selected to obtain reduced-order TPWL models. In this section, a range of results will be presented that demonstrate the effects of changing the number of linearization points, the number of reduced states, the snapshot ensemble used to create the POD basis, and the weighting procedure.

The POD basis calculation and the selection of linearization points can be performed efficiently using the same ensemble of snapshots. It is important that this snapshot selection span all operating conditions of interest. For the results presented here, three training trajectories were used, which corresponded to the three Gaussian input pulses given in Table 1. For each trajectory, snapshots were collected at every **Xth** timestep, yielding a total of **X** snapshots. POD basis vectors were then calculated, resulting in the POD eigenvalue spectrum plotted in Figure **??**. To capture 99%, 99.9%, and 99.99% of the snapshot energy defined by (6), **X,Y, and Z** basis vectors are required, respectively.

PLOT POD EVS HERE

By projecting each linearized model onto a sufficient number of POD basis vectors, accurate reduced-order models can be obtained; however, it should be noted that there are no accuracy or stability guarantees associated to these reduced models. The accuracy can be checked a posteriori by comparing the transfer functions of the full-order and reduced-order models at each linearization point. Figure **??** shows this comparison for the transfer function between an incoming density disturbance and the throat Mach number for one particular model. The reduced model uses **X** states, which corresponds to **X%** energy.

A FIGURE LIKE OLD FIG 13, BUT USE PROPER NUMBER OF STATES (50?). ALSO SHOULDN'T MATTER WHAT IS THE PERTURBATION SIZE/SHAPE - IT IS LINEAR AND YOU SHOULD BE USING FREQUENCY DOMAIN (SINUSOIDAL)? ARE YOU COMPARING LIN OR NONLINEAR CFD?

The second step in creating the reduced-order TPWL models is determine appropriate linearization points using Algorithm 1. GIVE SOME BRIEF RESULTS ABOUT NUMBER OF MODELS VS DELTAMIN. MAYBE A SMALL TABLE.

For each of the **X** selected linearization points, a reduced-order model was created by projection onto the reduced space spanned by the first **X** POD basis vectors. These models were then combined to form a TPWL system as defined by (16). Simulation results will be presented for the second weighting procedure given in Algorithm 2, which uses only the closest model.

Figures 10 and 11 present the simulation results for a range of different incoming density disturbances. For the Gaussian pulses in Figure 10, it can be seen that good agreement is achieved for the three training cases and for two intermediate cases not included in the snapshot collection. In Figure 11, the results for sinusoidal inputs are also very good.

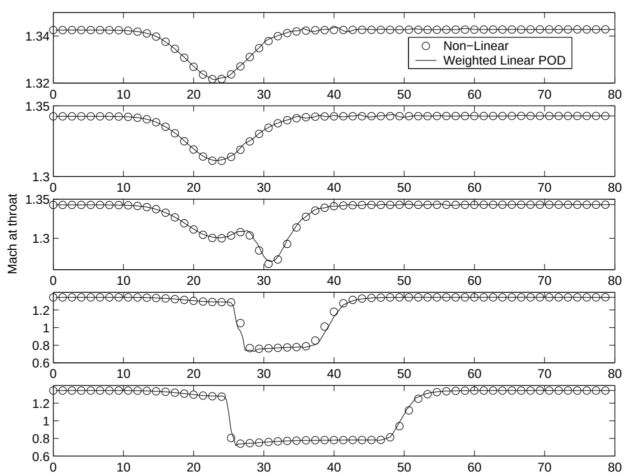

Fig. 10 POD method for various input. From top: Gaussian distribution of 1%, 1.5%, 2%, 2.5%, and 3% amplitude. 76 models with 50 states have been used. They have been created from three training trajectories using Gaussian distribution of 1%, 2% and 3% amplitude.

Table 4 presents a computational performance comparison between the nonlinear CFD, the full-order piecewise-linear and the reduced-order piecewise-linear methods. All algorithms were implemented in Matlab, except for the nonlinear solver, which was running under Fortran. The tests were performed in a Linux workstation with Pentium IV processor and 512MG Ram. The use-

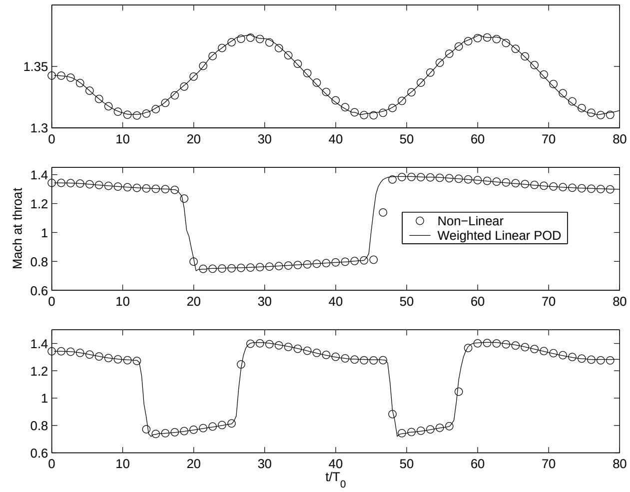

Fig. 11 POD method for various input. From top: Sinusoidal distribution of $\Lambda = 1.5\%$ $\omega_0 = 0.65$, $\Lambda = 2\%$ $\omega_0 = 0.35$ and $\Lambda = 3\%$ $\omega_0 = 0.65$. 76 models with 50 states have been used. They have been created from three training trajectories using Gaussian distribution of 1%, 2% and 3# amplitudes.

Nonlinear	Full Linear	Reduction	POD
2h 10 min	20 min	10 min	2 sec

Table 4 Comparison of the time involved in each methods.

fulness of POD can be seen immediately over the nonlinear CFD and the full-order linearized models. Also, its high computational speed allows a controller implementation. NEED TO SAY EXACTLY WHAT ARE THESE TIMES? FOR A SIMULATION? WHICH ONE?

References

[1]Berkooz, G., Holmes, P., Lumley, J., The Proper Orthogonal Decomposition in the Analysis of Turbulent Flows, Annual Review of Fluid Mechanics, vol. 25, pp. 539-75, 1993.

[2]Chen, Y., Model Order Reduction for Nonlinear Systems, M.S. Dissertation, MIT, Cambridge, MA, 1999

[3]Drela, M., Two-Dimensional Transonic Aerodynamic Design and Analysis using the Euler Equations. PhD thesis, Massachusetts Institute of Technology, 1985.

[4]Grimme, E. J., Krylov Projection Methods for Model Reduction, PhD Thesis,q University of Illinois at Urbana-Champaign, 1997.

[5]Hall, K. C., Thomas, J. P., Dowell, E. H., Reduced-order modelling of unsteady small-disturbance flows using a frequency-domain proper orthogonal decomposition technique, in Preceedings of the 37th Aerospace Sciences Meeting and Exhibit, AIAA Paper 99-0655, 199

[6]Hung, E., Yang, Y.-J., Senturia, S.D., Low-Order Models For Fast Dynamical Simulation of MEMS Microstructures, In Proceedings of the IEEE International Conference on Solid State Sensors and Actuators (Transducers '97), vol.2, 1997, pp.1101-04

[7]Kim, T., Frequency-Domain Karhunen-Loeve Method and Its Application to Linear Dynamic Systems, AIAA Journal, vol. 36, no. 11, pp. 2117-23, 1998

[8]Korenberg, M.J., Identifying Nonlinear Difference Equation and Functional Expansion Representations: the Fast Orthogonal Algorithm, Annals of Biomedical Engineering, vol.16, pp.123-42, 1998

[9]Korenberg, M.J., Hunter, I.W., The Identification of Nonlinear Biological Systems: Volterra Kernel Approaches, Annals of Biomedical Engineering, vol.24, pp.250-68, 1996

[10]Kowalski, M.E., Jin, J.-M., Karhunen-Loève Based Model Order Reduction of Nonlinear Systems, in Proceedings of the IEEE Antennas and Propagation Society International Symposium, vol.1, 2002, pp.552-5

[11]Lassaux, G., High-Fidelity Reduced-Order Aerodynamic Models: Application to Active Control of Engine Inlets, Masters Thesis, Dept. of Aeronautics and Astronautics, Massachusetts Institute of Technology, June 2002.

[12]Lau, T., Application of the Proper Orthogonal Decomposition to Slat Cove Noise Modeling, Master's thesis, Dept. of Aeronautics and Astronautics, Massachusetts Institute of Technology, June 2003.

[13]Lumley, J. L., The structure of inhomogeneous turbulent flow, Atmospheric Turbulence and Wave propagation (1967), 166-176.

[14]Mohammad, A.A., De Abreu-Garcia, J.A., A transformation approach for model order reduction of nonlinear systems, in Proceedings of the 16th Annual Conference of IEEE Industrial Electronics Society, vol.1, 1990, pp.380-3

[15]Paduano, J., Merchant, A., Drela, D., Lassaux, G., Schuler, B., Design and Testing of a High-Recovery, Actively Controlled Supersonic Inlet, Massachusetts Institute of Technology, 2002

[16]Phillips, J.R., Model Reduction of Time-Varying Linear Systems Using Approximate Multipoint Krylov-subspace Projectors, in Proceedings of the IEEE/ACM International Conference on Computer-Aided Design, 1998, pp.96-102.

[17]Phillips, J.R., Projection frameworks for model reduction of weakly nonlinear systems, in Proceedings of the 37th Design Automation Conference, 2000, pp.184-9

[18]Rewienski, M., White, J., A Trajectory Piecewise-Linear Approach to Model Order Reduction and Fast Simulation of Nonlinear Circuits and Micromachined Devices, in Proceedings of the International Conference on Computer-Aided Design, 2001, pp.252-7

[19]Rewienski, M., A Trajectory Piecewise-Linear Approach to Model Order Reduction of Nonlinear Dynamical Systems, PhD Thesis, Dept. of Electrical Engineering and Computer Science, Massachusetts Institute of Technology, June 2003.

[20]Willcox, K. E., Reduced-Order Aerodynamic Models for Aeroelastic Control of Turbomachines, PhD Thesis, Dept. of Aeronautics and Astronautics, Massachusetts Institute of Technology, February 2000.

[21]Willcox, K. E., Megretski, A., Fourier Series for Accurate, Stable, Reduced-Order Models for Linear CFD Applications, AIAA Paper 2003-4235, 15th Computational Fluid Dynamic Conference, Orlando, FL, June 2003.

[22]Willcox, K. E., Megretski, A., Model reduction for large-scale linear applications.

[23]Willcox, K. E., Paduano, J.D., Peraire, J., Hall, K.C., Low order aerodynamic models for aeroelastic control of turbomachines, in Proceedings of the American Institute of Aeronautics and Astronautics Structures, Structural Dynamics, and Materials Conference, vol.3, 1999, pp.2204-14

[24]Willcox, K. E., Peraire, J., Balanced Model Reduction via the Proper Orthogonal Decomposition, AIAA Journal, vol.40, no.11, pp.2323-30, 2002

[25]Zhang, Y., Henson, M.A., Kevrekidis, Y.G., Nonlinear model reduction for dynamic analysis of cell population models, Chemical Engineering Science, vol. 58, pp.429-45, 2003